Kastens, K. A., Mascle, J., et al., 1990
Proceedings of the Ocean Drilling Program, Scientific Results, Vol. 107

18. VOLCANICLASTIC SEDIMENTS IN THE TYRRHENIAN BASIN[1]

Floyd W. McCoy[2] and Winton Cornell[3,4]

ABSTRACT

The results of lithologic, petrographic, grain-size, and chemical studies of volcaniclastic sediments recovered during Leg 107 of the Ocean Drilling Program show that a variety of volcaniclastic sediments occur in the Tyrrhenian Basin. The abundance of volcanic glass and presence (or lack) of sediment structure is used to classify the sediments into four sediment-deposit types: (1) tephra fall, (2) volcaniclastic turbidite, (3) debris flow, and (4) volcanic sand. The abundance and distribution of these sediment types at Leg 107 sites are related both to proximity to volcanic sources and pathways of sediment transport to the basin floor.

Deposits directly related to volcanic events include tephra fall, debris flow, and some volcaniclastic turbidites. The latter are generated from reworking of tephra fall and from pyroclastic gravity flows that entered the sea at the time of (primary), or closely following (epiclastic), eruption. These turbidites occur throughout the basin, are glass-rich, and are most common in the central and southeastern portions of the basin. A large debris flow encountered at Sites 651 and 650 represents a marine-deposited equivalent of the Campanian Ignimbrite, a large pyroclastic deposit in the Phlegrean Fields produced about 38,000 yr ago. This correlation is confirmed by glass chemistry.

Volcanic sands and other volcaniclastic turbidites represent, on the other hand, deposits of more extensively reworked pyroclastics. Heterogeneous volcanic glass and mineral population, abundant detrital crystals, and, occasionally, high clay component attest to the secondary (epiclastic) origin of these deposits. Several large volcanic sands that occur immediately above vitric-rich layers may be derived directly from reworking of the vitric-rich layer, although predominantly in the nearshore and/or shelf environment.

Glass chemistry shows that volcaniclastic sediments at Leg 107 sites are mainly of local provenance. At westerly Sites 655 and 653 rhyolitic and trachytic glasses have a source in the nearby Pontine Archipelago. In the central part of the basin at Site 651, volcaniclastic sediments are primarily derived from the Campanian volcanic province. At southerly Site 650 provenance is mainly the Eolian Arc. Two major volcaniclastic turbidites at Site 650 contain calc-alkaline rhyolitic glass, documenting large eruptions of rhyolitic magma not before reported in the arc.

INTRODUCTION

Volcaniclastic debris forms a high proportion of the detrital component of sediments within back-arc basins, constituting as much as a third or a half of the sediment contribution (Klein, 1985). The influx of volcaniclastic material into marginal basins is controlled by both volcanic (primary) and secondary (epiclastic) processes (Fisher, 1984; Suthern, 1985); the resulting volcaniclastics can be used to characterize the history of volcanism within the adjacent magmatic provinces and to record changes in location, tempo, and style of sedimentary input of volcanic detritus into the basin (e.g., Sigurdsson et al., 1980). In addition, individual volcaniclastic layers (especially tephra falls) have proven valuable as correlative horizons within the pelagic stratigraphic record (e.g., Keller et al., 1978).

The Tyrrhenian basin is a back-arc basin within the complex geodynamic setting of the Mediterranean Sea (Kastens et al., 1988); it has developed behind the subduction plate-boundary between the European and African plates. An active volcanic belt (Eolian Arc) is present on the arcward edge of the basin. Bounding margins to the Tyrrhenian basin (the Sardinia continental margin and the Italian peninsular margin) have a complex history of magmatism (Fig. 1; DiGirolamo, 1978; Savelli, 1988).

Seven sites were drilled within the Tyrrhenian Sea during Leg 107 with the objective of better understanding the evolution of a back-arc basin within a complex zone of continental collision (Fig. 2). Positions and water depths of the sites, generalized lithologic logs, physiographic and tectonic setting, etc., are given in Kastens, Mascle, et al. (1987). In this study we report on volcaniclastic sediments encountered at each of these sites.

The major objectives of this study were to:

1. Identify the distribution and types of volcaniclastic sediments within the Tyrrhenian Basin,
2. Identify processes responsible for dispersing volcaniclastics to the basin, especially to central (e.g., Site 651) and southeastern (e.g., Site 650) portions of the basin where such sediments are recognized to be common (e.g., Paterne et al., 1986, 1988),
3. Correlate primary (i.e., directly related to a volcanic event) volcaniclastic layers (e.g., tephra fall layers) to terrestrial equivalents to supplement biostratigraphic studies,
4. Characterize the petrography and chemistry of volcaniclastics to establish provenance (e.g., Campanian province, Eolian Arc), and
5. Establish the temporal variation of influx of volcaniclastic sediment into the basin.

BACKGROUND

Processes of Volcaniclastic Sedimentation and Previous Studies in the Basin

Studies of composition, sedimentary structure, and facies distribution of volcaniclastic sediments in marginal basins demonstrate that this material is introduced by (1) primary deposition from volcanic events, and (2) secondary deposition by re-

[1] Kastens, K. A., Mascle, J., et al., 1990. *Proc. ODP, Sci. Results,* 107: College Station, TX (Ocean Drilling Program).
[2] Lamont-Doherty Geological Observatory of Columbia University, Palisades, NY 10964.
[3] Graduate School of Oceanography, University of Rhode Island, Narragansett, RI 02882-1197.
[4] Current address: Geological Survey of Canada, 601 Booth Street, Ottawa, Ontario, Canada K1A 0E8.

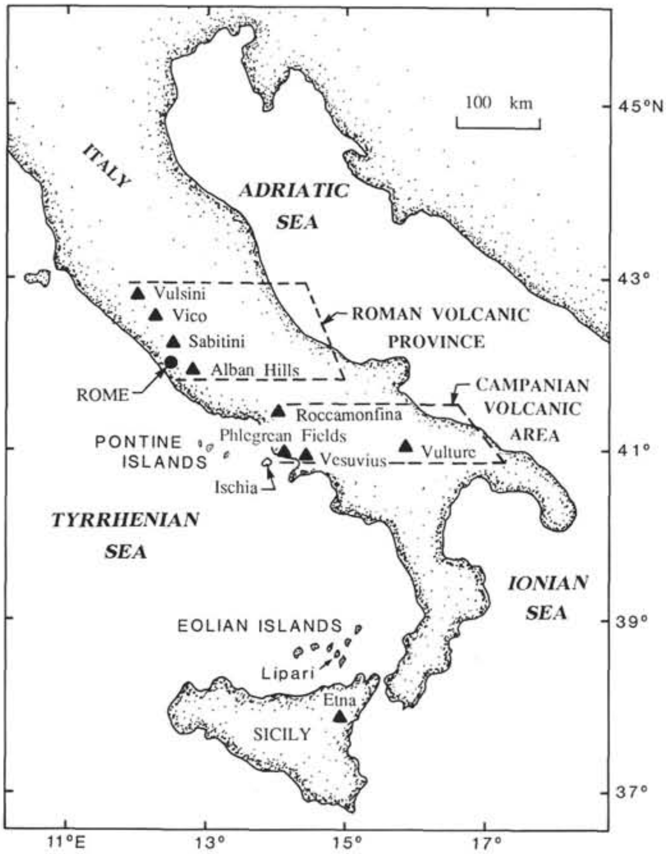

Figure 1. Geographical setting (after Gasparini et al., 1982) of the Roman, Campanian, and Eolian Arc volcanic provinces. Age of volcanism decreases to the south. Eolian Islands are the Neogene-aged expression of convergence of the European and African plates.

working of volcanic particles (Carey and Sigurdsson, 1984). Reworked volcanics are broadly classified as epiclastic sediments, and can encompass remobilized juvenile pyroclasts to subaerially (epigene) reworked and weathered material. Much of the volcaniclastic sediment introduced into marginal basins is coarse clastic detritus (Cas and Wright, 1987), although there are instances when it is extensively altered and/or weathered, yielding zeolites and clays that are proxies of a history of volcanism and sedimentation (Lee and Klein, 1986).

Primary Deposits

Those deposits that are considered primary can be divided into two broad classes: tephra fall and pyroclastic gravity-flow deposits. Tephra fall layers are common in marine sediments (e.g., Keller et al., 1978) and have been extensively used in stratigraphic studies. They are produced by dispersal of tephra in eruption plumes, with distribution over large areas (e.g., Ledbetter and Sparks, 1979). A primary tephra fall layer usually has few sediment structures other than size-grading. Secondary processes, however, can easily affect the ultimate form of the deposit on the seafloor (McCoy, 1980).

In the Mediterranean, explosive eruptions have been frequent, and a thorough documentation exists for such layers in marine sediments (Federman and Carey, 1980; Keller et al., 1978; Thunell et al., 1979). The Y-5 ash in the eastern Mediterranean is a good example (Cornell et al., 1983; Keller et al., 1978; Thunell et al., 1979). On the other hand, there are fewer tephra studies in the Tyrrhenian Sea (basin) and most are descriptive (Cita et al., 1981; Norin, 1958). It is only recently that a comprehensive tephrostratigraphy for late Pleistocene (< 80,000 yr) to Holocene sediments has been proposed (Paterne et al., 1986, 1988).

Volcanic eruptions also involve a number of pyroclastic gravity flow processes which generate a variety of deposits (Fisher and Schmincke, 1984). If entrance into water occurs, terrestrially-derived flows can undergo flow transformations (Fisher, 1984) to yield a spectrum of deposits that may differ considerably from their terrestrial counterparts. Such deposits are common in some back-arc basins (Sigurdsson et al., 1980). The paucity of examples of subaqueously-welded flows (Sparks et al., 1980; Wright and Mutti, 1981) is strong evidence that flows rarely maintain their original integrity in water. Some subaqueous volcaniclastic deposits can be correlated, however, to their contemporaneous subaerially-generated equivalents (Roseau deposit; Carey and Sigurdsson, 1980).

Secondary Deposits (epiclastic)

Reworking of subaerial and shallow-marine volcaniclastics through epiclastic processes introduces much volcaniclastic debris to the back-arc basin via debris flow, grain flow, and turbidity processes (Carey and Sigurdsson, 1984). Resulting deposits range from vitric-rich (e.g., Wright and Mutti, 1981), to crystal-dominated sands (Sigurdsson et al., 1980). Vitric-rich (enriched?) layers are often difficult to distinguish from layers formed by direct volcanic input (Wright and Mutti, 1981), and all gradations between vitric-rich epiclastic and eruption-generated deposits appear to exist (Fisher, 1984). Deposits of this type are common in Leg 107 sediments. In fact, most vitric-rich sediments we describe belong to this class of sediment.

It is a main conclusion of this paper that epiclastic processes dominate introduction of volcaniclastics into the Tyrrhenian back-arc basin. Similar conclusions were reached by Sarnthein and Bartolini (1973) and Bartolini et al. (1974) in their studies of several pumice-containing turbidites in Tyrrhenian deep-sea cores.

Sources of Volcaniclastic Sediment to the Tyrrhenian Basin

Magmatism within the Tyrrhenian area (Tyrrhenian Sea and adjacent land masses) has been active since at least the late Oligocene, and has been subdivided into five major episodes (Savelli, 1988). Of these, the four most recent (8.5–6.5 Ma; 5.5–1.8 Ma; 1.9–1.3 Ma; and 1.3 Ma to present) encompass the age-range (Tortonian to present) of sediments recovered in Leg 107 drill cores (Kastens, Mascle, et al., 1987). Most volcaniclastic material in Leg 107 cores is Pliocene or younger in age (this study; Kastens et al., 1988).

Composition of volcanic products during this time interval is quite diverse (DiGirolamo, 1978; Savelli, 1987, 1988). Two major provenances for volcaniclastics, however, can be identified within the circum-basin region.

The active arc of the Eolian islands and related seamounts is a province of calc-alkaline and shoshonitic volcanics. In addition to several major subaerial centers, an arcuate trend of seamounts extends toward the Italian margin as far as Palinuro seamount. The large Marsili seamount is often included in the province because of recent capping by calc-alkaline lavas (Colantoni et al., 1981). Oldest dated calc-alkaline activity in the arc is 1.3 Ma (Sisifo seamount; Beccaluva et al., 1981). Most pyroclastic deposits appear to be young, although knowledge of these deposits is limited to subaerial exposures. A typical example is the pyroclastic sequence on Lipari described by Crisci et al. (1983), produced during hydromagmatic eruptions.

A second major source are the Tuscan, Roman, and Campanian magmatic provinces that lie along the eastern border of the Tyrrhenian Sea on peninsular Italy (Fig. 1). Volcanism is oldest

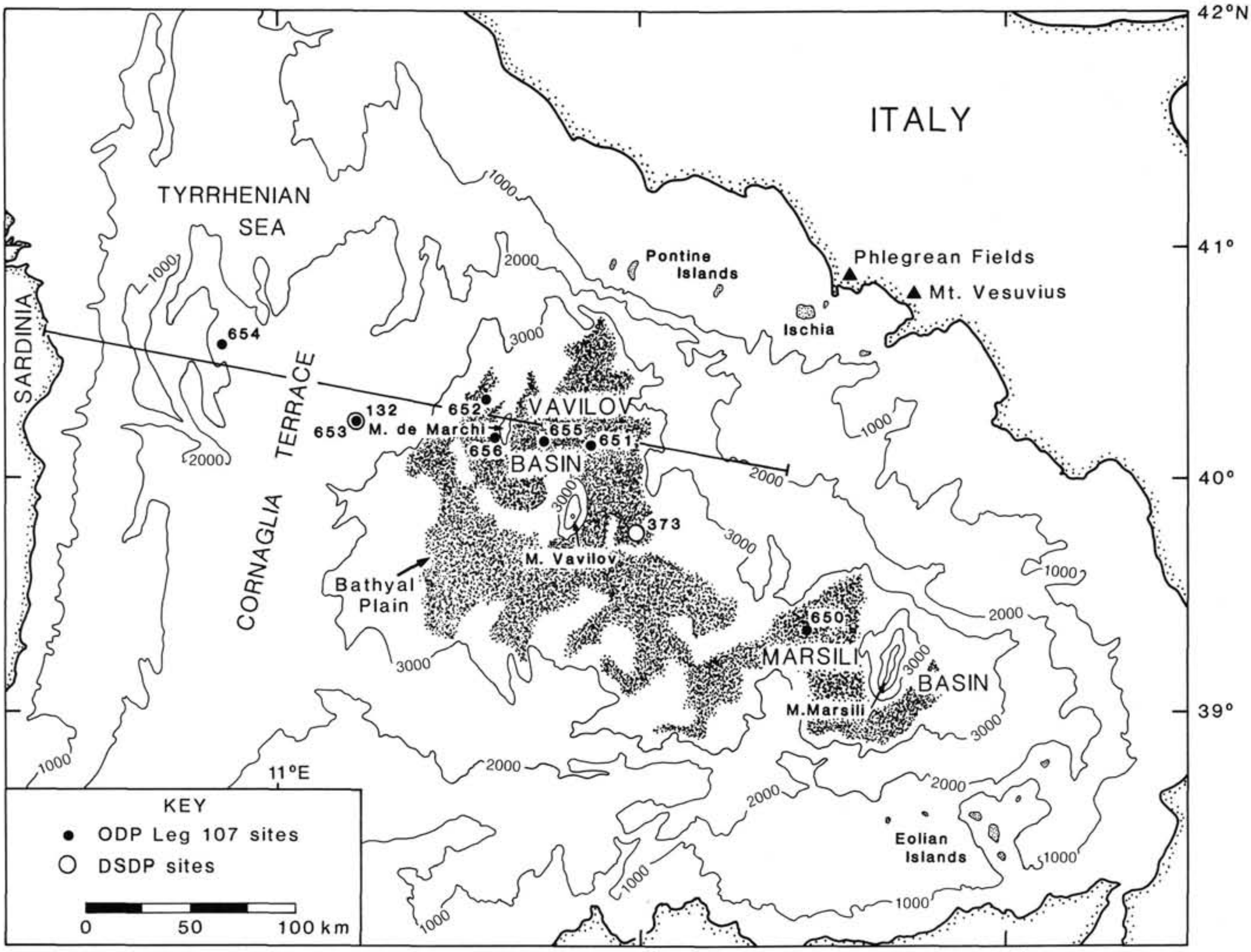

Figure 2. Location map of the Tyrrhenian Sea from Kastens et al. (1988). Shaded area is the bathyal plain. Leg 107 sites lie along a west-northwest to east-southeast transect, with exception of the more southerly location of Site 650. DSDP Sites 132 and 373 also given for reference.

in northern portions (Tuscan province; primarily 4.3–2.3 Ma) and youngest in southern portions (Campanian province). Pyroclastic material is particularly characteristic of Roman and Campanian volcanism and is represented by two major compositional series subdivided on the basis of K_2O content and degree of silica-saturation (DiGirolamo, 1978). A trachybasalt to trachyte series includes several large-volume (>tens of cubic kilometers of magma) ignimbrite deposits (Rosi et al., 1983; Sparks, 1975). A leucitite to phonolite series is represented by smaller volume (several cubic kilometers) Plinian deposits (Lirer et al., 1973; Sigurdsson et al., 1985).

LABORATORY METHODS

All cores from Sites 650 and 651 were redescribed, as were selected cores from Sites 652, 653, 654, 655, and 656. Descriptions reported for the cores in Tables 1 and 2 are based upon this reappraisal, and in many instances differ from those generated at sea and published in Kastens, Mascle, et al. (1987).

Petrographic observations were made to estimate modal proportions of glass and minerals. Estimates of component abundances were combined with a more limited smear-slide data set reported in Kastens, Mascle, et al. (1987). These data (Tables 1 and 2) have been used to assign sediment class types (see below).

A limited set of grain-size measurements were made by wet-sieving to examine variations in size-frequency in vertical profiles through several major volcaniclastic turbidites (see definition below) and several smaller vitric-rich layers. These data are reported in Table 3.

Chemical analysis for major and minor oxides in glass shards and minerals was made using a JEOL electron-probe microanalyzer at the University of Rhode Island (URI). Operating conditions were 125 nA beam current and 30 s counting times for all elements. Standard correction procedures for major and minor elements were those of Bence and Albee (1968). The Na-decay correction method of Nielsen and Sigurdsson (1981) was applied to compensate for beam-induced migration of Na during analysis of the glass shards. A standard empirical correction (URI lab) was applied to compensate for concomitant gain in Si and Al count rates for some glasses.

DEFINITIONS OF DEPOSIT TYPES

For the purpose of this study, layers containing 30 volume percent (%, herein) or more of pumice, glass shards, and volcanic minerals (retaining subhedral to euhedral outlines) were considered to be volcaniclastic layers. These layers have been subdivided into four sediment-deposit classes (tephra fall, volcaniclastic turbidites, debris flows, volcanic sands) based on the proportion of vitric material and types of sedimentary structure. The terminology we have chosen is similar to that utilized by Sigurdsson et al. (1980).

Tephra falls are distinguished by a minimum vitric fraction of 50% (usually >75%), sharp lower contacts with host sediment (no evidence of scour), limited size-grading and, most importantly, low levels (<10%) of debris indicative of a nonprimary volcanic origin. The nonprimary debris includes rounded mineral grains and displaced (from shallow water) microfossils and plant debris. Layers fitting this class are not as numerous as might be expected (compare Paterne et al., 1986, 1988), likely due to reworking and redeposition of many tephra to produce layers we designate as volcaniclastic turbidites. Layer 006, Hole 650A is a representative vitric-rich tephra fall (Table 1).

The volcaniclastic turbidites can be distinguished from tephra fall by having (1) an admixture of nonvolcanic components, (2) a lower percentage of volcaniclastic detritus (but not always), (3) sharp (scoured?) contacts with host sediment, and (4) the presence of Bouma units. A type example of this class of deposit is layer 036, Hole 650A.

Subaqueous volcanic debris flow as a class of sediment deposit is rare (Table 2). Coarse grain-size and massive sediment units contrast debris flows with volcaniclastic turbidites. Similarity to volcaniclastic turbidites is maintained in the high volcanic component, occasional sediment intervals with Bouma-type structures and inverse-grading of pumices. The type example of this class of deposit is layer 027, Hole 650A (Table 2).

Volcanic sands have the lowest volcanic component. Vitric fraction is less than 30%, but more than the 5%–10% minimum vitric component concentration we use to classify sediment units as detrital sands. Volcanic crystals are abundant (usually >25%). Because of their high crystal content, volcanic sands are better size-sorted than the volcaniclastic turbidites, yet have many of the same sediment structures. Some units are massive and may have been emplaced as grain flows.

It is also important to mention another class of sediments that is common in the cores, especially at Sites 650 and 651. These are the detrital sands, sediments that have up to 10% glass (more commonly, 5%), but are dominated by crystals. Although many crystals are volcanic in origin they are rounded, implying an energetic reworking history. Other studies (e.g., Sigurdsson et al., 1980) have considered similar units to be volcaniclastic sediments; however, we do not. A few occurrences are noted in Table 2 for comparative purposes.

Many layers in the cores contain zeolites in relatively high abundances (Tables 1 and 2). We presume zeolites to represent altered vitric material. Thus, most zeolite-rich layers are classed as tephra fall. Those that are thicker than 10 cm have been classified as volcaniclastic turbidites (Table 2).

RESULTS

Tephra Fall Layers

The order of presentation follows the drilling transect across the basin as described in Kastens et al. (1988). Projection of the sites along this transect (Fig. 2) constitutes a northwest to southeast progression from sites least likely to receive tephra fall (654, 653, 652, 656, 655), to sites (651, 650) for which tephra fall (and other volcaniclastic layers) should be abundant (compare Paterne et al., 1986, 1988).

Sites 654, 653, 652, 656, and 655

These are relatively tephra-poor sites. A maximum of seven layers is found at Site 655. Paucity of tephra fall reflects both the distance of the sites from volcanic sources and their position relative to predominant directions of wind transport. Studies of tephra-producing eruptions in the Campanian province (a very likely source of Tyrrhenian tephra falls) document transport of pyroclasts to the east and southeast (Cornell et al., 1983; Sigurdsson et al., 1985), away from the location of these sites.

Table 1. Tephra layers.[a]

Core	Interval (cm)	Layer no.	Glass (%)	Sediment type	Comment
Hole 656A					
2R-6	120–122	001	40	tephra	50% xtals
4R-1	0–5	002	n.a.	tephra	25% zeolites
Hole 655A					
1H-1	53–56	001	n.a.	tephra?	rare pumice
1H-2	124–127	002	n.d.	tephra?	zeolitic
2H-2	15–16	003	n.a.	tephra	60% zeolites
4H-4	50–53	004	55	tephra	>5% zeolites
5H-6	143–145	005	45	tephra	15% zeolites
8H-4	90–99	006	35	tephra	20% zeolites
8H-5	16–22	007	25	tephra	20% zeolites
Hole 654A					
2CC	8–10	001	>40	tephra	30% xtals
3R-1	20–23	002	55	tephra	25% xtals
38R-2	48–48.5	003	n.a.	tephra	zeolite-rich
38R-2	60–62	004	n.a.	tephra	zeolite-rich
39R-2	118–120.5	005	90	tephra	
Hole 653A					
2H-1	147–148	001	90	tephra	
3H-1	95–100	002	60	tephra	
5H-1	41.5–42.5	003	n.a.	tephra?	some pumice
6H-2	109–109.5	004	80	tephra?	zeolitic
Hole 653B					
2H-2	117–118	001	>60	tephra	
7H-5	90–97	002	>75	tephra	xtals w/glass
Hole 652A					
1R-1	109–110	001	n.a.	tephra?	glass lamina
1R-3	21–23	002	75	tephra	
1R-3	37–39	003	n.a.	tephra?	glass lamina
2R-1	50–60	004	n.a.	tephra?	zeolite-rich?
2R-3	90–97	005	>50	tephra	
Hole 651A					
24R-1	58–58.5	001	n.a.	tephra	zeolite-rich
24R-1	103–104	002	n.a.	tephra	zeolite-rich
25R-1	33–33.5	003	n.a.	tephra	zeolite-rich
25R-1	35–35.5	003	n.a.	tephra	zeolite-rich
25R-1	46.5–47	004	n.a.	tephra	zeolite-rich
25R-1	81.5–82	005	n.a.	tephra	zeolite-rich
25R-1	112–112.5	006	n.a.	tephra	zeolite-rich
25R-2	55.5–59.5	007	n.a.	tephra	zeolite-rich
25R-2	136–137	008	n.a.	tephra	zeolite-rich
25R-5	71	009	90	tephra	
27R-2	39–42	010	>80	tephra	disturbed
27R-3	21–23	011	n.a.	tephra	zeolite-rich
28R-2	64.5–66	013	n.a.	tephra	zeolite-rich
32R-1	0–7	014	n.a.	tephra?	sparse pumice
35R-1	0–2	015	n.a.	tephra	zeolite-rich
35R-2	141–141.5	016	n.a.	tephra	zeolite-rich
35R-3	6–6.5	017	n.a.	tephra	zeolite-rich
35R-3	31–31.5	018	n.a.	tephra	zeolite-rich
35R-3	57.5–59.5	019	n.a.	tephra	zeolite-rich
35R-3	112–112.5	020	n.a.	tephra	zeolite-rich
38R-1	38–42	021	n.a.	tephra	zeolite-rich
Hole 650A					
1H-1	20–21	001	>75	tephra	pod of ash
2H-1	146–147	002	85	tephra	
8H-5	107–110.5	003	>75	tephra	xtals at base
10H-2	19.5–20	005	>75	tephra	
10H-2	124–126.5	006	80	tephra	xtals w/glass
10H-4	129–136	007	95	tephra	weak grading
21X-3	11–15	008	n.a.	tephra?	rare pumices
22X-1	80.5–84.5	009	n.a.	tephra	zeolite-rich
22X-1	87.5–90	010	n.a.	tephra	zeolite-rich

Table 1 (continued).

Core	Interval (cm)	Layer no.	Glass (%)	Sediment type	Comment
Hole 650A (Cont.)					
22CC	26–29	011	n.d.	tephra	zeolitic
35X-1	116–122.5	012	n.a.	tephra?	large shards
48X-4	78–89	013	40	tephra	zeolitic
48X-5	28–37	014	<10	tephra	zeolitic
48X-6	82–85	015	50	tephra	zeolitic
48X-6	140–144	016	<5	tephra?	zeolitic
50X-6	36	017	20	tephra?	relict glass?
54X-3	107–109	018	>75	tephra	
54CC	14–14.5	019	>75	tephra	
55X-2	5–5.5	020	n.a.	tephra?	glass lamina
57X-2	109–114	021	70	tephra	plagioclase

[a] Column titles are: Core, refers to core and section numbers; Interval, interval in cm for the layer; Layer no., the sequential number of a layer at a given site; Glass, modal volume percent of glass; n.d., not determined; n.a., not applicable, which is the case for zeolite-rich layers in which volcanic glass is now represented by zeolites; Sediment type, refers to sediment type, with layers not meeting all guidelines outlined in the text noted as "tephra?"; Comment, miscellaneous comments on the layer; xtal, crystals.

None of the tephra fall layers are particularly thick, most are between 0.5 and 3 cm in thickness with the larger ones measuring near 10 cm. The five layers with thicknesses of 5 cm or more are found at Sites 652, 656, and 655 which are considerably east-southeast of westerly Sites 653 and 654. Although their position is proximal to a possible Campanian source area, the age and major element chemistry of the tephra falls (and some volcaniclastic turbidites; see later section) indicate a possible source within the Pontine Islands (Table 4).

It is common for the tephra fall at these sites to contain zeolites, either in combination with glass (e.g., Site 655) or as zeolite-only layers (e.g., Site 654). In most cases, zeolites occur in the oldest (based solely on stratigraphic position) tephra fall at a given site. An exception is Site 655 for which zeolites are pervasive. The thin Pleistocene sequence at this site (Kastens, Mascle, et al., 1987), however, demonstrates that zeolitic tephra here are as old as occurrences at other sites. Adoption of these zeolite-rich layers as tephra fall is cautionary, as it is difficult to characterize the layers because of fine grain-size, lack of sediment structure, and the fact that glass precursors are not always present. Preferential development of zeolites in glass-containing layers as opposed to siliciclastic layers (e.g., detrital sands) in the cores is strong evidence, however, that vitric layers are required precursors.

A few tephra fall layers are thin laminae of pumice (or shards) and may represent accumulations from pumice rafts. Such layers may be particularly widespread (McCoy, 1980). We note them here because of the rarity of megascopic tephra layers at these sites, identifying them in the comment column of Table 1 as "tephra?".

Sites 651 and 650

In contrast to the more western sites, tephra fall layers are more abundant at Sites 651 and 650 (Table 1). Most are in cores from deep levels (>200 m) in the Pleistocene sequence at each site. The paucity of tephra falls in the upper 200 m of sediment reflects our constraints on what constitutes a tephra fall layer. There are many vitric-rich layers within the upper 200 m of sediment at Sites 651 and 650 (Table 2), but pervasive development of sediment structures in these layers (some of which must be tephra falls) places them within the classification of volcaniclastic turbidites.

Table 2. Volcaniclastic turbidites, volcanic sands, and debris flows.[a]

Core	Interval (cm)	Layer no.	Glass (%)	Sediment type	Comment
Hole 656A					
5R-4	130–150	001	5	volc turb	5% zeolites
5R-5	0–28	001	n.a.	volc turb	zeolite-rich
Hole 655A					
5H-5	23–98	001	65	volc turb	2 glasses
Hole 653A					
2H-6	136–150	001	>50	volc turb	
2H-7	11–24	001?	n.a.	volc turb	
7H-1	41–42.5	002	20	volc sand	45% xtals
Hole 653B					
2H-3	79–82	001	60	volc turb	20% clay
2H-4	90–107	002	45	volc turb	50% xtals
6H-2	30–110	003	80	volc turb	clay clasts
6H-2	125–150	004	20	volc sand	
6H-3	0–7	004	n.a.	volc sand	
6H-3	72–112	005	>20	volc turb?	
7H-5	7–60	006	90	volc turb	laminations
Hole 652A					
1R-1	106–107	001	10	volc sand	80% xtals
1R-2	70–78	002	5	volc sand?	40% xtals
2R-1	130–150	003	10	volc sand?	25% xtals
7R-2	34–35	004	5	volc sand?	60% xtals
Hole 651A					
3R-1	40–60	001	5	volc sand?	thickness?
4R-6	6–24	002	5	volc sand?	thickness?
4R-6	32–120	002	5	volc sand?	detrital xtals
4R-7	0–67	002	5	volc sand?	dominant over
4CC	0–10	002	5	volc sand?	volcanic xtals
7R-1	0–150	003	>50	volc dflow	pumice rich;
7R-2	0–141	003	n.a.	volc dflow	pumice are
7R-3	0–150	003	n.a.	volc dflow	inverse-graded
7R-4	0–61	003	n.a.	volc dflow	from base to
7RCC	0–12	003	n.a.	volc dflow	top of unit
8R-1	0–28	003?	>25	volc turb	pumice, scoria
8R-1	41–44	003?	n.a.	volc turb	present;
8R-1	55–56	003?	n.a.	volc turb	volcanic xtals
8R-1	66–79	003?	n.a.	volc turb	abundant.
8R-1	97–128	003?	n.a.	volc turb	
8R-1	138–150	003?	85	volc dflow	pumice-rich
8R-2	0–150	003?	85	volc turb	pumice-rich
8R-3	0–121	003?	85	volc turb	pumice-rich
8R-4	10–73	003?	85	volc turb	pumice-rich
8CC	0–16	003?	85	volc turb	pumice-rich
9R-1	3–82	003?	40	volc turb	glass variable
11R-1	1–150	004	<5	volc sand?	some pumice
11R-3	26–150	004	<5	volc sand?	volcanic xtals
11R-4	10–150	004	<5	volc sand?	volcanic xtals
11R-5	0–150	004	<5	volc sand?	volcanic xtals
11R-6	0–57	004	<5	volc sand?	volcanic xtals
11CC	0–10	004	<5	volc sand?	volcanic xtals
12R-1	5–7	004	<5	volc sand?	volcanic xtals
12R-1	17–48	004	<5	volc sand?	volcanic xtals
12R-1	78–89	005	n.d.	volc sand?	pumice-bearing
13R-1	0–57	006	n.a.	volc turb	pumice-bearing
13R-1	57–90	006	n.a.	volc turb	volcanic xtals
13R-1	90–150	006	n.a.	volc turb	volcanic xtals
13R-2	20–150	006	50	volc turb	volcanic xtals
13R-3	0–79	006	50	volc turb	volcanic xtals
13R-5	0–133	006	50	volc turb	volcanic xtals
13R-6	0–40	006	50	volc turb	volcanic xtals
13CC	0–7	006	50	volc turb	volcanic xtals
14R-1	0–150	006?	50	volc turb	pumice-bearing
14R-2	0–90	006?	n.a.	volc turb	pumice-bearing
14CC	4–6	006?	n.a.	volc turb	rare pumice
15R-1	0–150	006?	n.a.	volc turb	pumice-bearing
15R-2	0–34	006?	n.a.	volc turb	pumice-bearing
15CC	0–13	006?	n.a.	volc turb	pumice-bearing
22R-1	0–16	007	n.d.	volc turb?	green glass

Table 2 (continued).

Core	Interval (cm)	Layer no.	Glass (%)	Sediment type	Comment
Hole 651A (Cont.)					
23R-1	0–10	008	35	volc turb	indurated
23R-1	12–18	009	n.d.	volc turb?	indurated
25R-3	139–144	010	45	volc turb	leucite
27R-1	67–72	011	50	volc turb	beige-colored
30CC	0–10	012	85	volc turb	disturbed
34R-2	110–151	013	60	volc turb	laminations
34R-3	0–24	013	n.a.	volc turb	w/variety of
34CC	0–8	013	n.a.	volc turb	structures
35R-4	119–150	014	>50	volc turb	white-colored
35R-5	0–10.5	n.a.	volc turb		
35R-5	45–50	015	n.d.	volc sand?	abraded glass
Hole 650A					
1H-1	40–55	001	>5	volc sand	xtal-rich
1H-2	3–4	002	n.d.	volc sand	volcanic xtals
1H-2	25–46	003	n.d.	volc sand	volcanic xtals
1H-2	46–126	004	70	volc turb	
2H-1	0–59	005	85	volc turb	two glasses
2H-1	85–120	005?	80	volc turb	two glasses
2H-2	59–60	006	15	volc sand?	volcanic xtals
2H-2	76–96.5	007	5		volcanic xtals
2H-2	103–125	008	85	volc turb	size grading
2H-2	134–144	008?	80		beige-colored
2H-3	35–36	009	5	volc sand?	
2H-3	88–92.5	010	20	volc sand	volcanic xtals
2H-3	121–122	011	10	volc sand	volcanic xtals
2H-4	0–69	012	70	volc turb	rounded pumice
2H-4	103–107	013	10	volc sand?	
2H-5	3–10	014	65	volc turb	euhedral xtals
2H-5	14–39	015	10	volc sand?	
2H-5	50–50.5	016	15	volc sand	volcanic xtals
2H-6	13–149	017	10	volc sand	
2CC	10–13	017	20	volc sand	volcanic xtals
3H-1	0–50	017	n.a.	volc sand	disturbed
3H-1	114–116	018	20	volc sand	volcanic xtals
3H-1	142–145	019	5	detr sand	xtals rounded
3H-2	20–29	020	5	detr sand	xtals rounded
3H-3	11–12.5	021	20	volc sand disturbed	
3H-4	57–64	022	5	volc sand?	large shards
3H-5	35–87	023	5	detr sand	some pumice
3H-5	109.5–130	024	75	volc turb	two glasses;
3H-6	0–15.5	024?	n.a.	volc turb	laminations
4H-1	93–101	025	>25	volc turb?	volcanic xtals
4H-3	18–150	026	20	volc sand	pumice lamina;
4H-4	0–32	026	n.a.	volc sand	two glasses;
4H-5	0–150	027	95	volc dflow	1.7 cm pumice;
4H-6	0–150	027	n.a.	volc dflow	two glasses
4H-7	0–50	027	n.a.	volc dflow	two glasses
4CC	0–20	027	n.a.	volc dflow	two glasses
5H-1	0–150	027	85	volc dflow	two glasses
5H-2	0–150	027	85	volc dflow	two glasses
5H-3	0–150	027	n.a.	volc dflow	two glasses
5H-4	0–1	027	n.a.	volc dflow	two glasses
5H-4	125–133	027	n.a.	volc turb	type Bouma
5H-4	133–142.5	027?	n.a.	volc turb	sequence;
5H-5	0–1	027?	n.a.	volc turb	volcanic xtals
5H-5	1–26	027?	>75	volc turb	are abundant
6H-4	5–150	027?	n.a.	volc turb	two glasses;
6H-5	0–150	027?	55	volc turb	glass encloses
6H-6	0–150	027?	n.a.	volc turb	clinopyroxene;
6H-7	0–53	027?	n.a.	volc turb	many euhedral
6CC	0–15	027?	n.a.	volc turb	volcanic xtals
7H-1	0–150	027?	n.a.	volc turb	volcanic xtals
7H-2	0–150	027?	n.a.	volc turb	volcanic xtals
7H-3	0–127	027?	>30	volc turb	volcanic xtals
7CC	0–20	027?	n.a.	volc turb	volcanic xtals
8H-1	0–150	027?	>50	volc turb	volcanic xtals
8H-2	0–150	027?	n.a.	volc turb	volcanic xtals
8H-3	0–120	027?	>50	volc turb	volcanic xtals
8H-3	120–145	027?	n.a.	volc turb	volcanic xtals
8H-4	0–34	027?	>50	volc turb	volcanic xtals

Table 2 (continued).

Core	Interval (cm)	Layer no.	Glass (%)	Sediment type	Comment
Hole 650A (Cont.)					
8H-4	83.5–93.5	027?	n.a.	volc turb	two glasses
8H-4	93.5–147	027?	>50	volc turb	
8H-5	27–38	028	10	volc sand	xtals at base
8H-5	70–97.5	029	>5	detr sand?	
9H-1	0–150	030	10	volc sand	two glasses
9H-2	0–150	030	n.a.	volc sand	>20% volcanic
9H-3	0–68	030	25	volc sand	xtals, mostly
9H-3	68–80	030	n.a.	volc sand	at base
9H-3	93–141	031	75	volc turb	
9H-3	141–150	031	n.a.	volc turb	
9H-4	0–17	031	n.a.	volc turb	
9H-4	28–132	032	10	volc sand?	>10% xtals?
10H-4	99–113	033	n.d.	volc sand?	
12H-1	0–150	034	55	volc turb	glass abundant
12H-2	0–150	034	45	volc turb	at top of unit
12H-3	0–150	034	n.a.	volc turb	volcanic xtals
12H-4	0–150	034	50	volc turb	mostly at base
12H-5	0–150	034	n.a.	volc turb	two glasses
12H-6	0–150	034	n.a.	volc turb	two glasses
12H-7	0–26	034	25	volc turb	two glasses
12CC	0–12	034	n.a.	volc turb	two glasses
13H-1	0–150	034	25	volc turb	>50% volcanic
13H-2	0–150	034	n.a.	volc turb	xtals; many
13H-3	0–150	034	20	volc turb	xtals here
13H-4	0–150	034	30	volc turb	xtals here
13H-5	0–150	034	n.a.	volc turb	xtals here
13H-6	0–106	034	30	volc turb	xtals here
13CC	0–9	034	n.a.	volc turb	xtals here
14CC	0–15	034	25	volc turb	xtals here
17X-1	75–120	035	>30	volc turb	xtals at base
26X-1	41–149	036	80	volc turb	glass-enriched
26X-2	0–150	036	n.a.	volc turb	at top;
26X-3	0–120	036	n.a.	volc turb	xtal-enriched
26X-4	0–131	036	n.a.	volc turb	at base
26CC	0–25	036	n.a.	volc turb	036 at base
27X-1	0–67	036	40	volc turb	at base
31X-1	8–16	037	55	volc turb	angular xtals
33CC	0–23	038	25	volc sand?	>15% xtals
35CC	0–33	039	30	volc turb?	>10% xtals
37X-1	0–150	040	35	volc turb?	>10% xtals
37X-2	0–23	"	n.a.	volc turb	>10% xtals
37CC	0–40	"	n.a.	volc turb	>10% xtals
42X-1	0–23	041	n.d.	volc sand	>50% xtals
42X-1	31–31.5	042	n.d.	volc turb?	zeolite lamina
55X-1	57–69	043	40	volc turb	angular xtals

[a] Column headings as in Table 1; individual sediment types are abbreviated as follows: volc turb, volcaniclastic turbidite; volc sand, volcanic sand; detr sand, detrital sand; volc turb? or volc sand?, indicates layer name is unsure, though it is likely this; volc dflow, volcaniclastic debris flow; n.a., same as in Table 1 for zeolitic layers, but also used for layers (e.g., Site 650, layer 034) for which modal proportions are determined at varying intervals rather than at all levels in the deposit.

Most of the tephra falls at Sites 651 and 650 are thin (<4 cm). The thickest layer at each site is only 7 cm (Table 1). As is observed for tephra falls at Sites 654, 653, 652, 656, and 655, the pervasive development of zeolites makes grain-size and sediment structure largely indeterminant for most of the tephra falls. Vitric tephra falls do, however, sometimes show vertical size-grading and crystal concentrations at the base.

As at Sites 654, 653, 652, 656, and 655, zeolites are common. For example, at Site 651 all but three tephra are zeolite-rich. At Site 650 zeolites are not as abundant, yet about half of the tephra bear zeolites. The age of sediments at Sites 651 and 650 in which zeolitic tephra falls first occur appear to be comparable (NN20 biostratigraphic zone), although sediment ages are not well constrained at Site 650. Lee and Klein (1986) in a study of zeolites in volcaniclastic sediments from several western Pacific marginal basins have indicated that heat flow is the overwhelming influence in the timing of zeolite development. Among Leg 107 sites, zeolites seem to appear at an earlier age in Sites 651 and 650 sediments. Both sites are located in the younger parts of the Tyrrhenian, have basaltic basement at the base of the sediment column, and high heat flow (Della Vedova et. al., 1984; Hutchison et. al., 1985).

Volcaniclastic Turbidites, Volcanic Sands, and Debris Flows

The dominant volcaniclastic sediment identified in the basin is turbidite-deposited (Table 2). Layers that are vitric-rich are volcaniclastic turbidites; volcanic sands are crystal-rich. The frequency of both types of layers increases southeast along the drilling transect (Fig. 2) as the Campanian and Eolian volcanic areas are approached. Turbidite sequences are particularly abundant at Sites 651 and 650.

Sites 654, 653, 652, 656, and 655

Volcaniclastic turbidites and volcanic sands are relatively rare at these sites; one site has a single layer (655), one has two layers (656), and one (654) no layers at all. The highest concentration of layers is found for Hole 653B. Companion Hole 653A, less than 1 km away, shows a lower frequency.

For most sites, only one of the two sediment types occurs. For example, Hole 653B and Sites 656 and 655 bear only volcaniclastic turbidites. Hole 652A, on the other hand, seems to bear only volcanic sands. At Hole 653A, both types occur. The predominance of one layer over another at the various sites (holes) must be related to sediment source. Many vitric-rich (volcaniclastic) turbidites are likely to represent reworked tephra falls. The source for volcanic sands is not as obvious; they may be distal turbidite facies with sources quite remote.

Thickness of the two sediment types is also quite different. Volcanic sands do not exceed 30 cm in thickness, while volcaniclastic turbidites are up to 80 cm in thickness. The thickest volcaniclastic turbidite (Hole 653B) contains clay clasts, indicating either erosion or slumping of (hemi)pelagic sediments. A significant amount (20%) of clay is also included in a thin (3 cm) volcaniclastic turbidite, perhaps because it is at its distal reach.

Zeolites also occur in the turbidites. One volcaniclastic turbidite at Site 656 is zeolite-rich; tephra falls at a comparable stratigraphic level at this site also contain zeolites (Table 1). In contrast, the single volcaniclastic turbidite at Site 655 contains less zeolites and is more vitric-rich than associated tephra fall.

Sites 651 and 650

These sites have numerous volcaniclastic turbidites and volcanic sands (Table 2) as a result of their proximity to volcanic sources. Petrography and chemistry of the sediments indicate predominantly local provenance at each site. For Site 651 the major source is the Campanian volcanic province. At Site 650 the primary source is the Eolian Arc. Proximity for turbidite sequences is further indicated by the high proportion of clastic intervals (Ta, Tb, and Tc in Bouma's terminology) relative to mud intervals (Td and Te). For example, we estimate that about 75% of the cumulative thickness of the turbidites is represented by intervals Ta, Tb, and Tc at Site 650.

In addition to higher frequency, both average and maximum thickness of turbidite units at Sites 651 and 650 are much greater than at the other sites. Many turbidite units are greater than 1 m thick. True maximum thickness is difficult to determine though, as muds occurring between major turbidites could be Te units, rather than intervals of (hemi)pelagic sediments. True thicknesses are also difficult to determine because of nonrecovered sediment during coring.

Pumice is a common constituent of the volcaniclastic turbidites at Sites 651 and 650. All pumices show evidence of rounding suggesting that glass and crystals may have been liberated by abrasion of pumice during transport. This process could contribute many of the glass-coated crystals common to the volcaniclastic turbidites. Alternatively, glass coatings may indicate that the source volcanic sediments had a very limited or even no reworking history. This latter interpretation could link volcaniclastic turbidites directly to eruption events.

Size-grading (Table 3) and density-sorting (see section on glass compositions) of components are also common in volcaniclastic turbidites. Crystal concentrations occur at the base of Ta units and throughout the basal clastic units of some turbidites (see comment section of Table 2; Hieke et al., this volume). In turn, glass is often concentrated near the top of the turbidites (e.g., layer 034 in Table 2; Site 650). Sorting by density is also evidenced by inverse size-grading of pumices. Limited granulo-

Table 3. Grain-size data for Sites 655, 653, and 650.

Hole no.	Core and section	Interval (cm)	Passing sieve no.	Weight percent	Table and layer no.
650A	12H-2	68–70	>250	0.00	Table 2, #034
			>180	0.14	
			>125	1.35	
			<125	98.50	
650A	12H-4	69–71	>250	5.75	Table 2, #034
			>180	5.78	
			>125	18.78	
			<125	69.70	
650A	12H-6	19–21	>250	34.69	Table 2, #034
			>180	6.03	
			>125	13.79	
			<125	45.49	
650A	13H-2	48–52	>250	34.54	Table 2, #034
			>180	13.52	
			>125	23.64	
			<125	28.30	
650A	13H-4	48–52	>250	39.75	Table 2, #034
			>180	14.47	
			>125	19.49	
			<125	26.29	
650A	26X-1	19–21	>250	0.25	Table 2, #036
			>180	0.14	
			>125	3.46	
			<125	96.15	
650A	26X-1	33–35	>250	1.61	Table 2, #036
			>180	5.58	
			>125	17.59	
			<125	75.22	
650A	27X-1	65–67	>250	1.72	Table 2, #036
			>180	3.03	
			>125	6.91	
			<125	88.35	
650A	48X-5	33–37	>250	0.52	Table 1, #021
			>180	0.24	
			>125	0.03	
			<125	99.22	
653B	6H-2	73–75	>250	0.68	Table 2, #003
			>180	0.46	
			>125	0.28	
			>90	0.22	
			>63	0.11	
			<63	98.25	
653B	7H-5	95–97	>250	2.78	Table 1, #002
			>180	3.43	
			>125	7.65	
			>90	9.65	
			>63	13.00	
			<63	63.49	
655A	4H-4	95–97	>250	0.06	Table 1, #004
			>180	0.51	
			>125	1.75	
			<125	97.68	
655A	5H-5	64–66	>250	2.99	Table 2, #001
			>180	8.32	
			>125	23.09	
			<125	65.60	

metric data show that greater than silt-size sediment (>63 mm) is more abundant near the base of the turbidites than at upper levels (Table 3).

Turbidites that are classified as volcanic sands are numerous at both sites, but are more frequent at Site 650. The lower vitric content and higher crystal content of the volcanic sands relative to volcaniclastic turbidites indicates that vitric components have been preferentially fractionated. A high proportion (>80%) of the volcanic glass occurring in both volcanic sands and volcaniclastic turbidites is low density bubble-wall shards, material susceptible to hydrodynamic sorting. It would be useful to examine surface textures of glass from the volcanic sands and volcaniclastic turbidites for evidence of a reworking history.

The age of greatest frequency of turbidites at Sites 651 and 650 is broadly coincident, and can be defined on the basis of calcareous nannoplankton stratigraphy (Kastens, Mascle, et al., 1987). At Site 650, the majority of turbidites date from late Pleistocene (NN21) to present. At Site 651 the age-range encompassing most of the turbidites (first 20 cores) extends from late-middle Pleistocene (NN20/NN21) to present. Extrapolation of ages for individual major turbidites using biostratigraphic datums and sediment column thickness was not attempted. However, Heike et al. (this volume) utilize foraminifera to define an approximate age of 90,000 yr for a turbidite (our layer 034, Table 2) from Site 650.

Volcaniclastic Debris Flow

One major unit correlated between Sites 651 and 650 has the sediment features of a debris flow (Table 2). It is closer to source (see next section) at Site 651, and is represented in Table 2 by layer 003 at Site 651 and layer 027 at Site 650. At both sites it is difficult to determine true thickness because of incomplete recovery in some core sections. At Site 651 the layer probably encompasses all of Cores 7 and 8 and the top section of Core 9. The cumulative recovered thickness is over 10 m. At Site 650 the layer encompasses part of Cores 4 and 5. The cumulative recovered thickness is over 8 m. At Site 650 the layer likely continues as a volcaniclastic turbidite through Core 8. Correlation of the debris flow between the two sites is made on the basis of glass chemistry (next section).

The main characteristics that distinguish the debris flow from the turbidites are its massive sediment structure and extremely high glass and pumice contents. The debris flow is also typified by pumice-rich intervals. At Site 651, over 25 pumice diameters were measured from one of these intervals. Maximum diameter is 1.7 cm, with many pumices over 1 cm. As observed in volcaniclastic turbidites, these pumices are all well-rounded. The ease with which pumice is abraded during transport implies that rounding does not necessarily indicate great travel distance.

Major Element Chemistry of Glasses

Composition of glasses in layers from several sites was determined, mostly from the large volcaniclastic turbidites and debris flows found at Sites 651 and 650. These layers were emphasized because of the likelihood that they could correlate with major volcanic events. Representative glass compositions are reported in Tables 4, 5, and 6. All analyses are also depicted in a K_2O vs. SiO_2 plot (Fig. 3; Barberi et al., 1974). Analytical totals for trachytic and rhyolitic glasses are often low, reflecting hydration of the glasses, nondetermination of trace elements, Cl, and F, and, in some cases, noncorrection for beam-induced migration of alkalis (especially Na; see notes at bottom of tables).

Most glasses belong to the high-K calc-alkaline magma series, encompassing the full range from basalt to rhyolite (Fig. 3). Glasses of this series are encountered at Sites 655, 653, and 651, with rhyolites most common. At Site 651, only a debris flow has been analyzed and all glass is trachytic and belongs to an alkaline series. Rare glass encountered at Site 654 in a siliciclastic turbidite is a basaltic andesite (Table 4). Glasses are unique enough, in most cases, to allow general correlations to magmatic provinces.

Sites 655 and 653

The rhyolitic and trachytic glasses at Sites 655 and 653 are very similar to pyroclastics in the Pontine Archipelago (Table 4; Barberi et al., 1967; Savelli, 1987). For example, at Site 655 low FeO and CaO rhyolitic glass (layer 001, Table 2) is virtually identical to the older (4.4 Ma) rhyolites of Ponza. On the other hand, the glass is less like the younger (1.75 Ma), more FeO-rich and MgO- and CaO-poor rhyolites (Table 4). The age of 4.4 Ma for the Ponza rocks is, however, much older than the 3.4–3.6 Ma age defined for the sediment/basalt contact at this hole. The layer itself has an age of late Pliocene (>1.8 Ma; Kastens, Mascle, et al., 1987).

At Site 653 both rhyolitic and trachytic glasses occur. Rhyolitic glass in Core 7, Section 5 also most closely resembles the older rhyolite series of Ponza (comparative data not shown). The old age of Ponza rhyolites contrasts with a biostratigraphic age of about early Pleistocene (late NN19). The rhyolite is not correlative, however, with the layer at Site 655.

Glasses in Core 6, Section 3 for Hole 653B are both rhyolitic and trachytic in composition. Rhyolitic glass in this layer is virtually identical to that at Site 655. However, if biostratigraphic ages are correct (see Table 4), the layers can not be correlative. Site 653B trachytic glasses (layers 003 and 004, Table 2) are similar to trachytes of Ponza that have ages somewhat comparable to biostratigraphic age defined by the cores (Table 4). A mean age of 1.1 Ma has been determined for the trachytes of Ponza (Savelli, 1987), an age grossly similar to the early Pleistocene age defined by biostratigraphy (Kastens, Mascle, et al., 1987). The trachytic glasses from these two layers also appear to be identical in composition. Trachytic magmas identified at Ventotene in eastern Pontine Archipelago, have maximum ages near 0.80 Ma (Metrich et al., 1985). These are less viable correlatives, though, as the older exposed volcanics are predominantly lavas.

An important feature of the analyzed layers from Sites 655 and 653 is that each layer consists predominantly of one glass compositional type. Predominance of a single glass type suggests that the layers are closely linked to volcanic events, rather than later sedimentary events that mobilize diverse pyroclastics. Explanations for age differences between the possible correlative volcanic events and ages of the layers as defined by biostratigraphy include sources other than the Pontine Archipelago, inappropriateness of comparing glass and whole-rock data, limited knowledge of the submerged stratigraphy of Pontine volcanoes, and, possibly, poor biostratigraphic controls.

Sites 651 and 650

At these sites a wide range of glass composition occurs, even within single volcaniclastic layers (Fig. 3). At Site 650, for example, glasses encompass several magmatic series (Table 5). The diversity can be largely related to temporal evolution of magma compositions in the Eolian Arc (Beccaluva et al., 1985). Input from sources outside the arc may also play a role since tephra falls derived from the Campanian Province (Fig. 1) have been noted to be intercalated with local source pyroclastics on Salina Island (Keller, 1980).

Layer 034 at Site 650 exemplifies the compositional diversity that can be found within a single layer. Glasses in this turbidite, for example, span magma compositions ranging from basaltic-andesite to rhyolite (Table 5; Fig. 3). Rhyolite is most common. Some of the compositional variation (61%–67% SiO_2) occurs

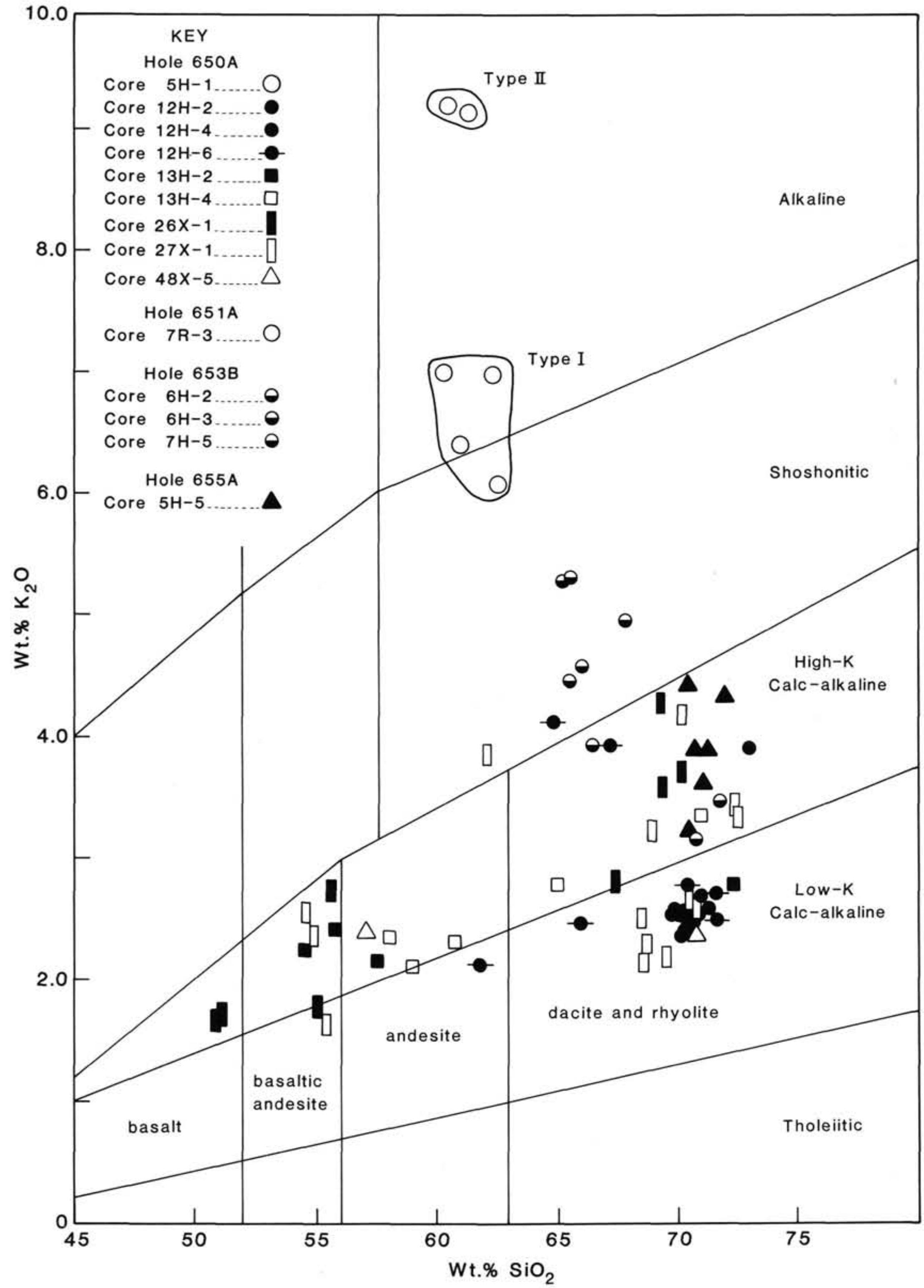

Figure 3. Plot of K_2O vs. SiO_2 for glasses from ODP Leg 107 volcaniclastic sediments. Values plotted are the nonnormalized (compare Tables 4, 5, and 6) data. Field boundaries adapted from Barberi et al. (1974).

within single microlite-rich pumices. Mafic and siliceous end-members, however, are homogeneous glasses. Persistence of $Na_2O > K_2O$ in the glasses in this layer over the compositional range of basalt to rhyolite is characteristic of the calc-alkaline series of Salina Island (Keller, 1980). Chemically-zoned pyroclastic sequences are known on Salina (Pollara sequence, 13,000 yr) in which the compositional range of andesite to dacite (whole-rock data) has been erupted in single volcanic events.

The large turbidite layer 036 at Site 650 is also compositionally diverse. Calc-alkaline glasses in this layer span basalt to

Table 4. Analyses of glasses from Sites 655 and 653.

Oxide	Hole 655A Core 5H-5	Hole 655A Core 4H-4	Hole 653B Core 7H-5	Type I Hole 653B Core 6H-3	Type II Hole 653B Core 6H-3	Hole 653B Core 6H-2	P-13 [a]rhyolite	P-39A [a]trachyte	PLM-2 [a]rhyolite
SiO_2	75.58	56.46	74.94	67.81	76.06	67.07	75.26	64.99	75.16
Al_2O_3	13.67	21.73	14.84	17.55	13.00	17.56	13.60	18.16	13.16
MgO	0.21	3.34	0.38	0.29	0.19	0.29	0.06	0.17	0.05
FeO	1.15	3.26	2.37	2.02	1.27	1.92	1.18	2.68	1.68
CaO	1.19	7.40	2.07	0.96	1.11	1.09	1.16	0.82	0.47
Na_2O	3.79	5.65	1.48	[b]6.48	[c]3.81	6.49	3.38	6.78	3.96
K_2O	4.17	1.81	3.50	4.23	[c]4.19	5.05	5.19	5.71	5.22
TiO_2	0.20	0.34	0.27	0.40	0.21	0.32	0.07	0.27	0.11
P_2O_5	0.01	0.00	0.09	0.13	0.11	0.09	0.03	0.04	0.01
MnO	0.02	0.01	0.05	0.13	0.05	0.12	0.04	0.18	0.08
Total	100.00	100.00	100.00	100.00	100.00	100.00	100.00	99.80	99.90
[d]Comment									
Si corr	no	no	no	no	no	no	n.a.	n.a.	n.a.
Na loss	yes	no	no	no	no	yes	n.a.	n.a.	n.a.
Total	93.93	96.72	95.17	97.66	93.55	97.63	94.60	99.80	99.90
Age	NN18–NN16	NN18–NN16	NN19	NN19	NN19	NN19	4.4 Ma	1.1 Ma	1.75 Ma
Deposit	volc turb	detr sand	tephra	volc turb?	volc turb?	volc turb	n.a.	n.a.	n.a.

[a] Analysis of P-13 from Barberi et al. (1967); analysis of P-39A is PNZ-39A from Savelli (1987), as is PLM-2; ages (Ma) are means from Savelli (1987).
[b] Value for Na_2O is from Hole 653B, 6H-3.
[c] Values of Na_2O and K_2O are from Hole 655A, 5H-5.
[d] Abbreviations are: Si corr, correction for Si-gain (see text) applied, yes or no?; Na loss, loss of Na determined (see text), yes or no?; Total, pre-normalization analytical total from probe analyses; Age, biostratigraphic zonation from Kastens, Mascle, et al. (1987), except Pontine Islands as above in [a].

rhyolite. Mafic glasses fall along the low-K/high-K calc-alkaline boundary, while rhyolites in this layer fall well within the (low-K) calc-alkaline field (Fig. 3). The basalts are strikingly similar to Keller's (1980) group average for high-Al basalts on Salina (Table 5).

A surprising feature of turbidites 034 and 036 at Site 650 is that major glasses in each appear to be identical (at the level of precision of the microprobe determinations). Two rhyolites (rhy-1 and rhy-2; see notation in Table 5) and a basaltic-andesite (bas-1) are indistinguishable. Rhy-1 and bas-1 have also been identified in zeolite-rich tephra fall layer 021 from Site 650.

Apparent repetition of glasses in these large turbidites and a tephra fall layer may be explained in several ways. For the turbidites, repetition could reflect reworking of volcanic material from a single source area, or even a single (major) pyroclastic sequence. Tephra fall, on the other hand, could be indicative of timing of the original volcanic event. Extensive development of zeolites in tephra fall 021 and not in turbidites 034 and 036 could be indicative of longer residence time of the tephra fall in the marine environment.

There is also evidence within turbidites 034 and 036 for systematic variation of relative abundance of major glasses with stratigraphic height. For layer 036, rhy-1, rhy-2, bas-1, and a basaltic glass are found at the base, rhy-1, rhy-2, bas-1, and andesitic glass are found at mid-level, while only rhy-1 and rhy-2 are found at upper levels. In layer 034 (Site 650), rhy-1, bas-1, and miscellaneous basaltic-andesite and dacite occur at the base, rhy-1 and miscellaneous andesitic to dacitic glasses occur at mid-level, while rhy-1 and rhy-2 only occur in upper levels. Hydrodynamic sorting dependent on density and shape differences between shards of basalt (dense, poorly vesicular) and rhyolite (less dense, vesicular) may account for vertical variation of glass compositional types in the turbidites. It is possible that all vitric-rich turbidites containing glasses of variable density show this feature.

The only layer that can be correlated on the basis of glass chemistry between sites is the volcaniclastic debris flow from Sites 651 (layer 003, Table 2) and 650 (layer 027, Table 2). The two trachytic glasses found in the debris flow and turbidite are identical to those reported for Y-5 ash (Table 6). The Y-5 layer has been identified as tephra fall related to the Campanian Ignimbrite, a large volcanic deposit dated at 38,000 yr (Thunell et al., 1979) with a source in the Phlegrean Fields area (Rosi et al., 1983) of mainland Italy. Thus the debris flow is the marine equivalent of the Campanian Ignimbrite, probably generated by slumping and reworking of tephra fall and pyroclastic gravity flows. Discharge of pyroclastic gravity flows directly into the sea during eruption is also likely to have been important. The source caldera is situated in the nearshore shallow marine environment (Rosi et al., 1983). Testing of this hypothesis will require better biostratigraphy for Sites 651 and 650 sediments.

Occurrence of the layer as a deposit with both turbidite and debris flow units is similar to facies variation described for the Roseau submarine pyroclastic debris-flow (Carey and Sigurdsson, 1980). Such facies variation may be the result of transformations in flow mechanisms (Fisher, 1984).

DISCUSSION

The results of our lithologic, petrographic, grain-size, and chemical studies of volcaniclastic sediments recovered during ODP Leg 107 drilling show that a variety of volcaniclastic sediments occur in the Tyrrhenian Basin. The abundance and distribution of these sediments shows strong regional variation.

The most important volcaniclastic deposit we identify in basin sediments is a large volcaniclastic debris flow. This sediment deposit occurs at Sites 651 and 650. The debris flow is interpreted to be a marine-deposited facies of the Campanian Ignimbrite (Barberi et al., 1978). Correlation to this major terrestrial deposit is confirmed by occurrence in the debris flow of two trachytic glasses of distinct composition, known to characterize the ignimbrite and associated tephra fall (Table 6; Cornell et al., 1979).

At Site 650 the debris flow is composed of two different volcaniclastic sediment-deposit types (Table 2, Fig. 4). The lower part of the deposit is a turbidite. The upper level of the deposit is a debris flow. Occurrence of a turbidite facies indicates effi-

Table 5. Analyses of glasses from Site 650.

Oxide	rhy-1[a] Hole 650A Core 12H-4	rhy-2[a] Hole 650A Core 12H-4	bas-1[a] Hole 650A Core 13H-2	rhy-1[a] Hole 650A Core 13H-4	andesite[b] Hole 650A Core 13H-4	dacite[b] Hole 650A Core 13H-4	rhy-1[a] Hole 650A Core 26X-1	rhy-2[a] Hole 650A Core 26X-1	bas-1[a] Hole 650A Core 27X-1	rhy-2[a] Hole 650A Core 27X-1	basalt Hole 650A Core 27X-1	rhy-1 Hole 650A Core 48X-4	bas-1 Hole 650A Core 48X-4	Sa-210[b] Keller Salina
SiO_2	72.29	74.35	55.98	72.07	59.99	65.34	72.03	75.11	56.47	74.03	51.57	72.67	57.48	51.34
Al_2O_3	14.09	14.00	15.15	14.13	15.00	13.85	13.81	13.81	15.59	14.48	16.63	13.62	15.95	17.00
MgO	0.58	0.32	3.74	0.56	2.57	1.32	0.60	0.31	3.87	0.31	6.21	0.56	3.62	6.75
FeO	3.00	1.48	9.91	3.09	8.48	6.74	3.22	1.58	9.35	1.56	8.38	3.63	8.63	9.00
CaO	2.17	1.25	7.57	2.44	6.10	4.32	2.32	1.35	7.62	1.28	11.61	2.18	7.45	10.80
Na_2O	4.48	4.20	3.54	4.39	3.94	4.26	4.78	3.84	3.31	3.80	2.85	3.98	3.15	2.16
K_2O	2.57	4.00	2.27	2.69	2.30	2.80	2.49	3.56	2.32	4.12	1.72	2.58	2.43	1.00
TiO_2	0.59	0.31	1.31	0.54	1.20	0.84	0.54	0.30	1.13	0.34	0.83	0.53	0.87	0.50
P_2O_5	0.09	0.03	0.30	0.05	0.30	0.38	0.15	0.12	0.20	0.03	0.10	0.14	0.29	0.17
MnO	0.12	0.07	0.24	0.03	0.12	0.14	0.06	0.02	0.12	0.05	0.10	0.10	0.13	0.18
Total	100.00	100.00	100.00	100.00	100.00	100.00	100.00	100.00	100.00	100.00	100.00	100.00	100.00	98.90
[c]Comment														
Si corr.	no	no	no	no	no	no	no	no	no	no	no	no	no	
Na loss	yes	yes	yes	yes	yes	yes	yes	yes	yes	yes	yes	yes	yes	
Total	97.96	98.15	100.02	96.25	98.83	99.47	96.04	96.38	98.10	94.07	98.30	97.21	99.15	
Age	NN21	NN21	NN21	NN21	NN21	NN21	NN19	NN19	NN19	NN19	NN19	NN19	NN19	
Sediment	volc turb	volc turb	volc turb	volc turb	volc turb	volc turb	volc turb	volc turb	volc turb	volc turb	volc turb	tephra	tephra	

[a] The progression for the first four columns of data is from upper (12H-4) to lower (13H-2, 13H-4) levels of turbidite 034; the progression for columns 7, 8, 9, and 10 is from upper (26X-1) to lower (27X-1) levels of layer 036; rhy-1 and rhy-2 are rhyolites, bas-1 is a basaltic andesite.

[b] Andesite and dacite are representative miscellaneous (and minor) glasses found in turbidite 034; basalt represents rare, mafic basalt glass. Sa-210 is basalt from Salina in Keller (1980).

[c] Same source as in Table 4.

Table 6. Analyses of glasses from Site 650 compared with Y-5 ash and Campanian Ignimbrite.

	Type I Hole 650A Core 5H-1	Type II Hole 650A Core 5H-1	Type I Hole 650A Core 7R-3	(glass) Y-5 ash[a]	(pumices) whole-rock Camp ign[a]	Type II Camp ign[b]
SiO_2	64.60	62.34	62.00	61.95	62.72	61.25
Al_2O_3	18.65	18.29	18.91	18.46	19.11	18.84
MgO	0.34	0.67	0.34	0.35	0.35	0.82
FeO	2.94	3.25	3.02	2.82	3.10	3.49
CaO	1.83	2.51	1.83	1.82	1.63	2.63
Na_2O	4.66	3.03	6.75	6.96	5.55	3.22
K_2O	6.28	9.30	6.52	7.26	7.08	9.41
TiO_2	0.44	0.37	0.48	0.37	0.46	0.34
P_2O_5	0.08	0.15	0.06	n.d.	n.d.	n.d.
MnO	0.18	0.09	0.09	n.d.	n.d.	n.d.
Total	100.00	100.00	100.00	100.00	100.00	100.00
[c]Comment						
Si corr	yes	yes	yes	no	n.a.	no
Na loss	no	no	yes	yes	n.a.	yes
Total	96.87	98.37	98.16	97.11	99.33	98.31
Age	NN21	NN21	NN20/NN21	38,000 yr	38,000 yr	38,000 yr
Sediment	volc dflow	volc dflow	volc dflow	n.a.	n.a.	

[a] Y-5 ash, from Federman and Carey (1980); Camp Ign represents the Campanian Ignimbrite of Barberi et al. (1978).
[b] Mafic trachytic scoria in Campanian Ignimbrite (Cornell et al., 1979).
[c] Age of the Y-5 ash and Campanian Ignimbrite are the biostratigraphic age of Y-5 ash from Thunell et al. (1979).

cient dilution of the volcanic component during transport. The transition to debris flow could have been controlled by a significant increase in the eruption-regulated supply rate of pyroclastic material to the basin. Limitations of biostratigraphy for Site 650 sediments makes it difficult to determine whether emplacement of the debris flow was contemporaneous with eruption. However, occurrence of the source caldera of the Campanian Ignimbrite in a nearshore shallow-water setting (Rosi et al., 1983) makes it very likely that deposition was contemporaneous with eruption.

The primary result of this study is the recognition that volcaniclastic turbidites are the predominant volcaniclastic sediment-deposit type within basin sediments. Although such deposits have been recognized before in basin sediments (e.g., Bartolini et al., 1974), this study is the first to document the abundance and temporal and regional variability of their occurrence.

Of the sites examined, Sites 651 and 650 show the greatest abundance of volcaniclastic turbidites. The high abundance at these sites reflects the fact that they are proximal to very active sources of the Eolian Arc and Campanian volcanic province, respectively. On the other hand, volcaniclastic turbidites at the other ODP Leg 107 sites are much less abundant. The most important feature of nearly all volcaniclastic turbidites is that the nonvolcanic components in the turbidites indicate that many are derived from, or have at least transected, shelf and other shallow-water environments (comment column of Table 2; Kastens, Mascle, et al., 1987; Hieke et al., this volume). The volcaniclastic turbidites incorporate these components and are introduced into basin sediments by several processes.

Some volcaniclastic turbidites are likely to represent contemporaneous marine equivalents of pyroclastic gravity flows that entered the sea. In this regard they have origins analogous to the debris flow correlated to the Campanian Ignimbrite. A few volcaniclastic turbidites may even be distal turbidite facies of deposits that are debris flows closer to source (hence, base of slope?). The very large turbidites 034 and 036 at Site 650 may be related to debris flows developed adjacent to the Eolian Arc. Belderson et al. (1974), for example, have noted that Eolian island submarine slopes are steep cones comprised of pyroclastic debris. Efficient transport of this material away from the islands appears to take place through submarine canyons prominent throughout the arc (Barone et al., 1982; Belderson et al., 1974). Canyons such as these would be ideal pathways to the basin for pyroclastic material.

Volcaniclastic turbidites produced from reworking of tephra falls could also be contemporaneous with eruption. Reworking would primarily take place by slumping from the steeper slopes of the basin. We expect turbidites of this origin to be common because numerous tephra falls have been identified in piston cores from various locations in the Tyrrhenian Basin (Paterne et al., 1986, 1988). Distinction between volcaniclastic turbidites related to reworking of tephra fall and those related to pyroclastic gravity flows would require very detailed paleontological work. On average, relatively deeper-water fossils might characterize volcaniclastic turbidites related to reworking of marine tephra falls. The scale of the turbidites related to either origin would not, however, necessarily be a useful criterion for deciphering the mechanism by which they were generated. Tephra falls in the Tyrrhenian Basin can range from a few centimeters to more than 50 cm in thickness (Cornell et al., 1983; Paterne et al., 1988), and thus reworking of tephra falls could generate turbidites of variable thicknesses.

Some volcaniclastic turbidites may be produced by reworking of pyroclastics between eruptions. This is not unexpected since repose periods between eruptions occupy the bulk of the time interval covering the history of a volcano (Cas and Wright, 1987). Volcaniclastic turbidites of this origin would be typified by low ($<50\%$?) glass contents, a heterogeneous volcanic mineral and glass population, glasses with abraded and pitted surfaces, and abundant detrital components. Several volcaniclastic turbidites from Sites 651 and 650 characterized by high abundances of both detrital crystals and volcanic crystals are likely to have this type of origin (Table 2).

Volcanic sands, on the other hand, especially at Sites 651 and 650, have likely accumulated through processes analogous to those generating sand turbidites and pebbly sands in the basin today. Several studies indicate, for example, that sediments we would describe as volcaniclastic turbidites and volcanic sands have been introduced to the basin through canyons on the Italian continental margin (Bartole et al., 1984; Bartolini et al., 1974). These layers appear to have been derived from sediments with a considerable history of reworking (Bartolini et al., 1974), as reflected by the texture and abundance of their volcanic components. Studies of gravity cores from the Gulf of Naples (and Pozzuoli) have shown that both primary and reworked pyroclastic (their terminology) layers are abundant nearshore of the Campanian volcanic province (Carbone et al., 1984). Transport of these sediments from the nearshore to the basin may be frequent during stormy periods (compare Sigurdsson et al., 1980).

Some of the larger volcanic sands, however, are closely related to volcaniclastic turbidites. For example, at Hole 651A a major volcanic sand immediately overlies the debris flow correlated to the Campanian Ignimbrite (Fig. 4). A thick volcanic sand also overlies the large volcaniclastic turbidite layer 006 at Hole 651A. Similarly, at Hole 650A volcanic sands occur immediately above volcaniclastic turbidite layers 004, 031, and possibly 034. In addition, a major volcanic sand occurs immediately above the debris flow (layer 027) at Hole 650A. Volcanic sands of this occurrence may be generated solely by reworking of the associated (underlying) volcaniclastic layers. Some sands may even be correlatable between sites. Although widespread sands may be formed *in situ* by the activity of bottom currents, it is more likely they are derived from reworking of pyroclastics in nearshore and shelf environments.

Determination of glass chemistry in the volcaniclastic layers has also provided important data regarding the origin of major layers. For example, glasses of rhyolitic composition characterize the large volcaniclastic turbidites 034 and 036 from Hole 650A, and document large eruptions of rhyolite previously unknown in the Eolian Arc. For both of these layers, the occurrence of rhyolitic glass with high Na_2O/K_2O, consistent $Na_2O > K_2O$ for glass ranging from basalt to rhyolite, and strong similarity of basaltic glass to the high-Al basalts in Keller's (1980) compilation is strong evidence that the eruptions may have originated on Salina.

Another result from glass chemistry is that dominant glasses in volcaniclastic turbidites 034 and 036 at Site 650 have identical compositions. One explanation that can be proposed for this

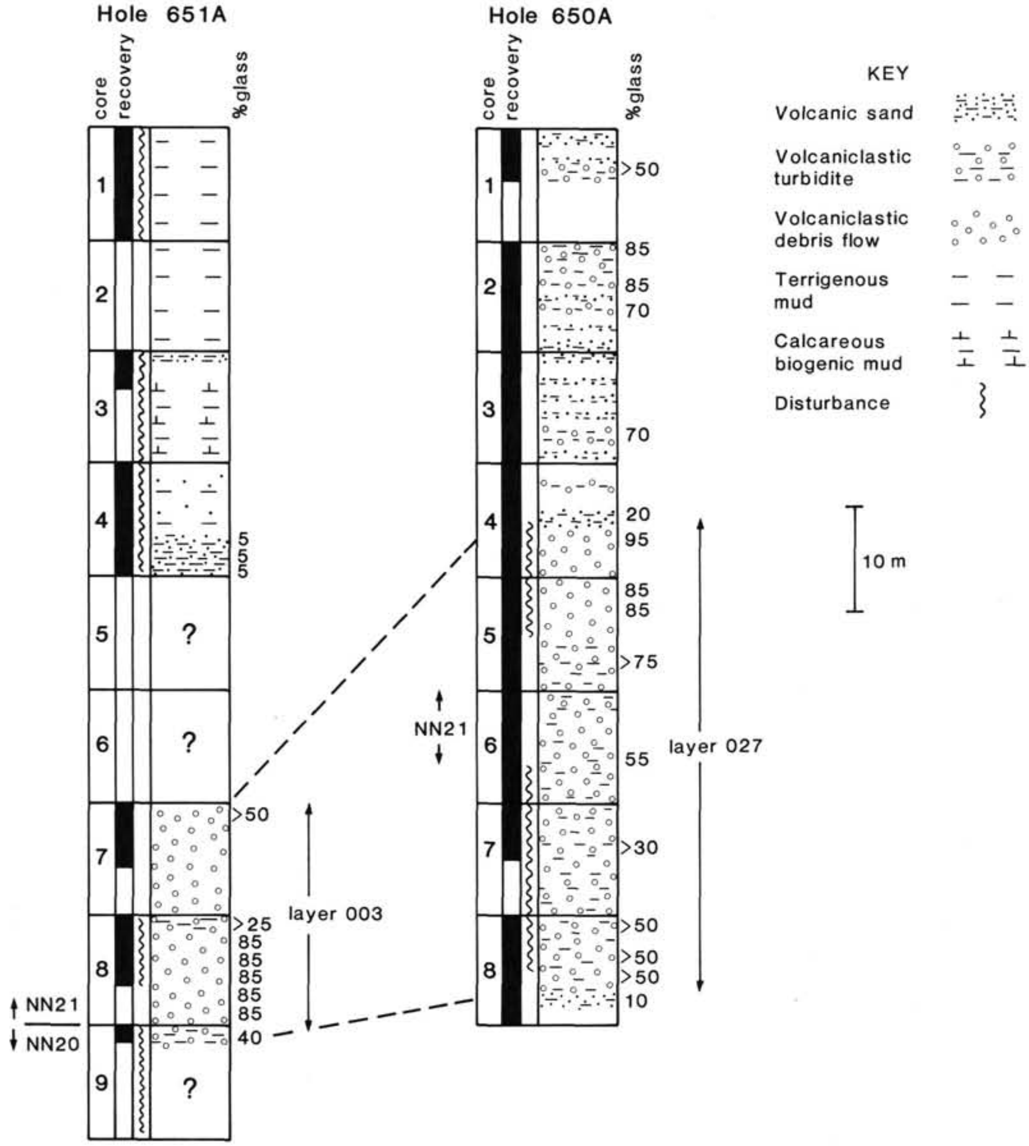

Figure 4. Diagrammatic lithologic section for debris flow and volcaniclastic turbidite correlated to the Campanian Ignimbrite. Sections are for Sites 651 and 650. Layer number next to each section is from Table 2. Also shown is volcanic sand that overlies the debris flow at each site.

occurrence is that layer 036 represents a deposit contemporaneous with eruption, and that layer 034 is the epiclastic equivalent of the associated terrestrial deposit, or even layer 036 itself. Higher modal contents of glass in layer 036 is consistent with this interpretation. Better biostratigraphic data are required, however, to define the age of these layers.

Unfortunately, very few of the layers we have examined can contribute to a tephrochronology for Leg 107 sediments. For example, correlation of tephra fall and volcaniclastic turbidites from Sites 653 and 655 to possible sources in the Pontine Archipelago (Barberi et al., 1967; Savelli, 1987) shows that terrestrial deposits of appropriate composition have ages that are different from biostratigraphically-defined ages for the marine layers (Kastens, Mascle, et al., 1987). At Sites 651 and 650 only, the debris flow can be correlated to a terrestrial deposit (the Campanian Ignimbrite). This correlation provides an age of 38,000 yr for the debris flow. Also at Site 650, an age of 90,000 yr for a turbidite has been assigned by Hieke et al. (this volume; our layer 034 in Table 2).

A chronology of volcaniclastic sedimentation for the Tyrrhenian basin may also be derived from study of Leg 107 sediments. For example, the frequency of volcaniclastic sediments vs. age reveals that volcaniclastic sediments become common in the late and middle Pleistocene. This occurrence is coincident both with volcanism in the Eolian Arc (1.3 Ma to present; Beccaluva et al., 1985) and in the Campanian Province (Savelli, 1988). Timing of input of the volcaniclastics relative to eruptions, sea-level stands, and tectonic history of the basin is, however, difficult to judge. The numerous raised beach terraces (Keller, 1980) on islands in the Eolian Arc demonstrate an active erosion history within the Eolian Arc and peri-Tyrrhenian area in general. Fluctuating sea level (the terraces), rapid subsidence of the basin (Kastens et al., 1988), and high rates of volcanism in the arc and on mainland Italy all have contributed to the high frequency and diversity of volcaniclastic sediments in the basin.

A model for volcaniclastic sedimentation in the Tyrrhenian basin therefore embraces minimal deposition for westerly Sites 656, 655, 654, 653, and 652, and high deposition rates in central and southern portions of the basin at Sites 651 and 650. Most layers at the westerly sites contain a single glass type, indicative of a genesis directly linked to a volcanic event, rather than epiclastic processes which mix pyroclastics of diverse origin. Mixing of this sort is, on the other hand, common at Sites 651 and 650. Site 650 especially shows that a wide range of glasses can occur in individual layers. Both Sites 651 and 650 also show a diversity of volcaniclastic sediment types, ranging from crystal-dominated volcanic sands to extremely vitric-rich volcaniclastic debris flows. Such diversity is to be expected in an environment where input from numerous sites occurs.

Seismic data provide supporting evidence for infilling of some parts of the basin by volcaniclastic sediments. In the southern part of the basin, for example, a sediment-wedge partly composed of volcaniclastics fills and caps small topographically-perched basins behind the Eolian arc (Barone et al., 1982). Infilling by volcaniclastic sediments in these basins postdates middle Pliocene (Barone et al., 1982). An apron of volcaniclastic sediments also surrounds and fills small basins adjacent to Ventotene and Ponza islands on the eastern edge of the central portion of the Tyrrhenian basin (Barberi et al., 1967; Zitellini et al., 1984). However, the age of infilling of these basins is not well defined.

CONCLUSIONS

Volcaniclastic sediments of considerable diversity are present within the Tyrrhenian basin. The diversity is greatest in southern portions of the basin where sources are numerous and have been active since the late to middle Pleistocene. Volcaniclastic sedimentation in this region of the basin appears to be analogous to that documented in other back-arc settings (e.g., Lesser Antilles Arc; Sigurdsson et al., 1980), although limited coverage by Leg 107 drilling does not allow for development of a comprehensive model of sedimentation in the basin.

An important result of this study is the recognition of several large volcaniclastic deposits previously undocumented in the basin. A volcaniclastic debris flow correlatable between Sites 651 and 650, some 150 km apart, is the marine equivalent of the 38,000 yr Campanian Ignimbrite of mainland Italy (Barberi et al., 1978; Thunell et al., 1979). Thick, vitric-rich volcaniclastic turbidites at Site 650 are likely to have been derived from major eruptions of rhyolite within the Eolian Arc. Such deposits have not yet been reported in terrestrial deposits in the arc. We suggest that source may be Salina island and that subsequent research for terrestrial correlatives of the marine layers should focus on this island.

The most common volcaniclastic sediments in the basin can be classified as volcaniclastic turbidites. These turbidites may have several origins, including generation from pyroclastic gravity flows entering the sea, reworking of tephra fall, and reworking of pyroclastics during the repose period between volcanic events. Volcaniclastic turbidites generated by the latter process can be distinguished from those generated by the former processes on the basis of heterogeneous glass and mineral population and textures of constituent volcanic components.

Volcanic sands in the basin are mainly derived from shelf- and nearshore-reworked pyroclastics. Some large volcanic sands, however, appear to be directly related to major volcaniclastic turbidites and debris flows. Their deposition shortly after related vitric-rich volcaniclastic layers reflects heavy sediment-loading on land and in the nearshore and shelf regions caused by eruptions.

Finally, tephrochronology is difficult for Leg 107 sediments. Volcaniclastic turbidites and tephra falls from western Sites 653 and 655 have compositional equivalents in the Pontine Archipelago (Savelli, 1987), but sediment ages are different than age of the volcanics. At southern sites, especially Site 650, biostratigraphy is too limited to confidently define ages of the layers. When datable (e.g., layer 034; Hieke et al., this volume), terrestrial correlatives do not exist. Hope for developing a comprehensive tephrochronology rests with better biostratigraphy combined with radiometric dating of layers, and in further field studies within the Eolian Arc.

ACKNOWLEDGMENTS

Comments by S. Carey were particularly helpful, as were reviews by K. Kastens, M. Cita, J. Mascle, and W.B.F. Ryan. We also wish to thank D. Browning for his help with sample preparation, petrography, grain-size analyses, and microprobe analyses. Financial support for this study was provided by USAAC.

REFERENCES

Barberi, F., Borsi, S., Ferrara, G., and Innocenti, F., 1967. Contributo alla conoscenza vulcanologica e magmatologica delle isole dell'Arcipelago Pontino. *Mem. Soc. Geol. It.,* 6:581–606.

Barberi, F., Innocenti, F., Ferrara, G., Keller, J., and Villari, L., 1974. Evolution of Eolian arc volcanism (southern Tyrrhenian Sea). *Earth. Planet. Sci. Lett.,* 21:269–276.

Barberi, F., Innocenti, F., Lirer, L., Munno, R., and Pescatore, T., 1978. The Campanian ignimbrite: a major prehistoric eruption in the Neapolitan area (Italy). *Bull. Volcanol.,* 41:1–22.

Barone, A., Fabbri, A., Rossi, S., and Sartori, R., 1982. Geological structure and evolution of the marine areas adjacent to the Calabria Arc. *Earth Evol. Sci.,* 3:207–221.

Bartole, R., Savelli, D., Tramontana, M., and Wezel, F. C., 1984. Structural and sedimentary features in the Tyrrhenian margin off Campanian, south Italy. *Mar. Geol.,* 55:163–180.

Bartolini, C., De Giuli, C., and Gianelli, G., 1974. Turbidites of the southern Tyrrhenian Sea. *Boll. Soc. Geol. It.,* 93:3–22.

Beccaluva, L., Gabbianelli, G., Lucchini, F., Rossi, P., Savelli, C., and Zeda, O., 1981. Magmatic character and K/Ar ages of volcanics dredged from the Eolian seamounts (Tyrrhenian Sea). *In* Wezel, F. (Ed.), *Sedimentary Basins of Mediterranean Margins*: Bologna (C.N.R. Italian Project of Oceanography, Tecnoprint), 361-368.

Beccaluva, L., Gabbianelli, G., Lucchini, F., Rossi, P., and Savelli, C., 1985. Petrology and K/Ar ages of volcanics dredged from the Eolian seamounts: implications for the geodynamic evolution of the Calabrian Arc. *Earth Planet. Sci. Lett.*, 74:187-208.

Belderson, R. H., Kenyon, N. H., and Stride, A. H., 1974. Features of submarine volcanoes shown on long range sonographs. *J. Geol. Soc. Lond.*, 130:403-410.

Bence, A. E., and Albee, A. L., 1968. Empirical correction factors for electron microanalysis of silicates and oxides. *J. Geol.*, 76:382-403.

Carbone, A. Lirer, L., and Munno, R., 1984. Caratteri petrografici dei livelli piroclastici rinvenuti in alcuni gravity cores nel Golfo di Pozzuoli e nel Golfo di Napoli. *Mem. Soc. Geol. It.*, 27:195-204.

Carey, S., and Sigurdsson, H., 1980. The Roseau ash: deep-sea tephra deposits from a major eruption on Dominica, Lesser Antilles Arc. *J. Volcanol. Geothermal Res.*, 7:67-86.

Carey, S., and Sigurdsson, H., 1984. A model of volcanogenic sedimentation in marginal basins. *In* Kokelaar, B. P. and Howells, M. F. (Eds.), *Marginal basin geology: Volcanic and associated sedimentary and tectonic processes in modern and ancient basins*: London (Blackwell Scientific Publications), 37-58.

Cas, R.A.F., and Wright, J. V., 1987. *Volcanic Successions, Modern and Ancient*: London (Allen and Unwin).

Cita, M. B., McCoy, F. W., and Paggi, L., 1981. Tephrachronology of the Mediterranean deep-sea record; new data from the western Mediterranean Ridge and from the Tyrrhenian Basin. *Rend. Soc. Geol. It.*, 4:255-258.

Colantoni, P., Lucchihi, F., Rossi, P., Sartori, R., and Savelli, C., 1981. The Palinuro volcano and magmatism of the southeastern Tyrrhenian Sea (Mediterranean). *Mar. Geol.*, 39:M1-M12.

Cornell, W. C., Sigurdsson, H., and Sparks, R.S.J., 1979. The Campanian Ignimbrite, Diversity of glass composition: evidence for a mixed-magma eruption. *Trans. Am. Geophys. Union*, 60:409.

Cornell, W. C., Carey, S. N., and Sigurdsson, H., 1983. Computer simulation of transport and deposition of the Campanian Y-5 ash. *J. Volcanol. Geothermal Res.*, 17:89-109.

Crisci, G., Delibrias, G., de Rosa, R., Mazzuoli, R., and Sheridan, M., 1983. Age and petrology of the late Pleistocene brown tuffs on Lipari, Italy. *Bull. Volcanol.*, 46: .

Della Vedova, B., Pellis, G., Foucher, J. P., and Rehault, J. P., 1984. Geothermal structure of the Tyrrhenian Sea. *Mar. Geol.*, 55:271-289.

Di Girolamo, P., 1978. Geotectonic settings of Miocene-Quaternary volcanism in and around the eastern Tyrrhenian Sea border (Italy) as deduced from major element geochemistry. *Bull. Volcanol.*, 41-3: 229-250.

Federman, A. N., and Carey, S. N., 1980. Electron microprobe correlation of tephra layers from eastern Mediterranean sediments and the island of Santorini. *Quat. Res.*, 13:160-171.

Fisher, R. V., 1984. Submarine volcaniclastic rocks. *In* Kokelaar, B. P., and Howells, M. F. (Eds.), *Marginal basin geology: Volcanic and associated sedimentary and tectonic processes in modern and ancient basins:* London (Blackwell Scientific Publications), 5-27.

Fisher, R. V., and Schmincke, H.-U., 1984. *Pyroclastic Rocks*. Berlin (Springer-Verlag).

Gasparini, C., Iannacone, I., Scandone, P., and Scarpa, R., 1982. Seismotectonics of the Calabrian Arc. *Tectonophysics*, 84:267-286.

Hutchison, I., Von Herzen, R., Louden, K., Sclater, J., and Jemsek, J., 1985. Heat flow in the Balearic and Tyrrhenian basins, Western Mediterranean. *J. Geophys. Res.*, 90:685-701.

Kastens, K., Mascle, J., et al., 1987. *Proc. ODP, Init. Repts.*, 107: College Station, TX (Ocean Drilling Program).

Kastens, K., et al., 1988. ODP Leg 107 in the Tyrrhenian Sea: insights into passive margin and back-arc basin evolution. *Geol. Soc. Am. Bull.*, 100:1140-1156.

Keller, J., 1980. The island of Salina. *In* Villari, L. (Ed.), *The Eolian Islands: An Active Arc in the Mediterranean Sea*. Rend. Soc. It. Mineral. Petrol., 36:489-524.

Keller, J., Ryan, W.B.F., Ninkovich, D., and Altherr, R., 1978. Explosive volcanic activity in the Mediterranean over the past 200,000 years as recorded in deep-sea sediments. *Geol. Soc. Am. Bull.*, 89: 591-604.

Klein, G. deV., 1985. The control of depositional depth, tectonic uplift, and volcanism on sedimentation processes in the backarc basins of the western Pacific. *J. Geol.*, 93:1-25.

Ledbetter, M., and Sparks, R.S.J., 1979. Duration of large-magnitude explosive eruptions deduced from graded bedding in deep-sea ash layers. *Geology*, 7:240-244.

Lee, Y., and Klein, G. deV., 1986. Diagenesis of sandstones in the back-arc basins of the western Pacific Ocean. *Sedimentology*, 33:651-675.

Lirer, L., Pescatore, T., Booth, B., and Walker, G.P.L., 1973. Two plinian pumice-fall deposits from Somma-Vesuvius, Italy. *Geol. Soc. Am. Bull.*, 84:759-772.

Metrich, N., Santacroce, R., and Savelli, C., 1985. *Ventotene, a Quaternary potassic alkaline volcano in central Tyrrhenian Sea: geochemistry, mineral chemistry and K/Ar geochronology*. Abstract of meeting of Soc. It. Mineral. Petrol.

McCoy, F., 1980. The upper Thera (Minoan) ash in deep-sea sediments: distribution and comparison with other ash layers. *In* Doumas, C. (Ed.), *Thera and the Aegean World, II*: London, 57-78.

Nielsen, C. H., and Sigurdsson, H., 1981. Quantitative methods for electron microprobe analysis of sodium in natural and synthetic glasses. *Am. Mineral.*, 66:547-552.

Norin, E., 1958. The sediments of the central Tyrrhenian Sea; Sediment Cores from the Mediterranean and Red Sea. *Swed. Deep-Sea Repts.*, 5:287-334.

Paterne, M., Guichard, F., Labeyrie, J., Gillot, P. Y., and Duplessy, J. C., 1986. Tyrrhenian Sea tephrochronology of the oxygen isotope record of the past 60,000 years. *Mar. Geol.*, 72:259-285.

Paterne, M., Guichard, F., and Labeyrie, J., 1988. Explosive activity of the south Italian volcanoes during the past 80,000 years as determined by marine tephrochronology. *J. Volcanol. Geothermal Res.*, 34:153-172.

Rosi, M., Sbrana A., and Principe, C., 1983. The Phlegrean Fields: structural evolution, volcanic history and eruptive mechanisms. *J. Volcanol. Geothermal Res.*, 17:273-288.

Sarnthein, M., and Bartolini, C., 1973. Grain size studies on turbidite components from Tyrrhenian deep sea cores. *Sedimentology*, 20: 425-436.

Savelli, C., 1987. K/Ar ages and chemical data of volcanism in the western Pontine Islands (Tyrrhenian Sea). *Boll. Soc. Geol. It.*, 106:537-546.

________, 1988. Late Oligocene to Recent episodes of magmatism in and around the Tyrrhenian Sea: implications for the processes of opening in a young inter-arc basin of intra-orogenic (Mediterranean) type. *Tectonophysics*, 146:163-181.

Sigurdsson, H., Sparks, R.S.J., Carey, S. N., and Huang, T. C., 1980. Volcanogenic sedimentation in the Lesser Antilles Arc. *J. Geol.*, 88: 523-540.

Sigurdsson, H., Carey, S., Cornell, W., and Pescatore, T., 1985. The eruption of Vesuvius in A.D. 79. *Nat. Geogr. Res.*, 1:332-387.

Sparks, R.S.J., 1975. Stratigraphy and geology of the ignimbrites of Vulsini volcano, central Italy. *Geol. Rundsch.*, 64:497-523.

Sparks, R.S.J., Sigurdsson, H., and Carey, S. N., 1980. The entrance of pyroclastic flows into the sea, II. theoretical considerations on subaqueous emplacement and welding. *J. Volcanol. Geothermal Res.*, 7: 97-105.

Suthern, R. J., 1985. Facies analysis of volcaniclastic sediments: a review. *In* Brenchley, P. J., and Williams, B.P.J. (Eds.), *Sedimentology, Recent Developments and Applied Aspects*: Oxford (Blackwell Scientific), 123-146.

Thunell, R., Federman, A., Sparks, S., and Williams, D., 1979. The age, origin and volcanological significance of the Y-5 ash layer in the Mediterranean. *Quat. Res.*, 12:241-253.

Wright, J. V., and Mutti, E., 1981. The Dali ash, Island of Rhodes, Greece: a problem in interpreting volcanigenic sediments. *Bull. Volcanol.*, 44:153-167.

Zitellini, N., Marani, M., and Borsetti, A. M., 1984. Post-orogenic tectonic evolution of Palmarola and Ventotene basins (Pontine Archipelago). *Mem. Soc. Geol. It.*, 103:121-131.

Date of initial receipt: 10 November 1988
Date of acceptance: 12 February 1989
Ms 107B-119